Comparison of recent dynamic subgrid-scale models in turbulent channel flow

By H. Jeanmart † AND G. S. Winckelmans †

Some recent subgrid-scale models are evaluated in turbulent channel flow at $\mathrm{Re}_\tau = 395$. The models considered were chosen among those performing best in decaying isotropic turbulence, following the study by Winckelmans & Jeanmart (2001): the dynamic Smagorinsky model (used as a baseline); a dynamic and regularized version of the variational multiscale model of Hughes, Mazzei, Oberai & Wray (2001); a dynamic "Smagorinsky + hyperviscosity" model (here with two dynamic coefficients); and a dynamic Smagorinsky model acting on an artificially-enhanced velocity field. The last three models put more emphasis than the Smagorinsky model on the subgrid-scale (SGS) dissipation at small scales, leading to significant improvement of the results in isotropic turbulence. The last two models combine viscosity and hyperviscosity effects.

The dynamic procedure was implemented for each model, with and without adding a test projection in the wall-normal direction. The projection uses a combined "sampling + interpolation" procedure, applied in physical space.

The models are assessed and compared to the direct numerical simulation (DNS) data of Moser, Kim & Mansour (1999) on the basis of mean profiles of velocity, rms velocities and reduced (deviatoric) turbulence intensities. A main outcome is the good behavior of the multiscale model of Hughes *et al.* as compared to the Smagorinsky model. Good results are also obtained when using the Smagorinsky model acting on an artificially-enhanced velocity field. In all cases, the dynamic procedure without test "sampling + interpolation" in the wall-normal direction leads to better agreement with the DNS data. The poor performance of "sampling + interpolation" is most probably due to the interpolation part, and a possible solution to the problem is proposed.

1. Introduction

The practical approach to large-eddy simulation (LES) is concerned with modeling the effective "subgrid-scale" stress (SGS stress) due to the projection from the complete u_i field to the incomplete large-eddy field $\widetilde{u}_i$: a non-regular operation, the effect of which must be modelled. On the other hand, the mathematical approach usually assumes a regular explicit filter: a regular convolution acting on u_i to produce the filtered field $\overline{u}_i$, leading to an effective "subfilter-scale" stress (SFS stress). One can also consider practical LES with regular filtering added to the projection, thus solving for $\overline{\widetilde{u}}_i$ instead of $\widetilde{u}_i$. The effective stress is then the sum of a SFS stress (which can be reconstructed) and a SGS stress (which must be modelled).

A systematic comparison of many of the recent LES models and approaches was conducted by Winckelmans *et al.* (2001a) for the case of decay of isotropic turbulence (48^3 LES started from a truncated 256^3 DNS). The models tested were:

† Center for Systems Engineering and Applied Mechanics (CESAME), Université Catholique de Louvain, Belgium

- viscosity model (Smagorsinky (1963));
- mixed "Smagorinsky + hyperviscosity" models (similar to the model proposed in Métais *et al.* (1992), but formulated differently and with only one coefficient);
- the variational multiscale model, Hiughes *et al.* (2001a) (basically the Smagorinsky model applied to half of the wavenumbers, from $k_{\max}/2$ to $k_{\max}$);
- the Smagorinsky model acting on an artificially-enhanced velocity field (a new model);
- the approximate-deconvolution model (ADM), Stolz *et al.* (1999), Stolz *et al.* (2001).

The spectral behavior of the models was investigated numerically. Two diagnostics were used: the model dissipation spectrum and the energy spectrum. This systematic comparison work pointed out the superiority of the models combining viscosity and higher order viscosity. Models that behave as viscosity at low k and-higher order viscosity at high k can indeed reproduce the correct dissipation spectrum for the SGS stress. The best results were those with "viscosity + k^6 hyperviscosity" (also consistent with the findings reported by Métais *et al.* (1992)). The model by Hughes *et al.* performs better than the Smagorinsky model (even though it lacks the part of the SGS dissipation that occurs at low wavenumbers). The Smagorinsky model acting on an artificially-enhanced velocity field also leads to better results than the standard Smagorinsky model (Smagorsinky (1963)).

Another conclusion of this investigation was the possible uselessness, at least in pseudo-spectral methods, of using additional explicit filtering, thus requiring "deconvolution" methods augmented by "regularization" terms: either the method used in Winckelmans *et al.* (2001b) or that used in Stolz *et al.* (1999), Stolz *et al.* (2001): the results are, at best, equivalent to (and usually worse than) those obtained from LES without additional explicit filtering, using the Smagorinsky model.

LES with added explicit filtering is not considered here. The purpose of this work is to study the SGS models in a more challenging test case, the turbulent channel flow (here at $\mathrm{Re}_\tau = 395$) to see if the conclusions from isotropic turbulence still hold. All models are implemented in their dynamic version (Germano *et al.* (1991), Ghosal *et al.* (1992), Ghosal *et al.* (1995)). A more consistent test projection operator for the wall-normal direction is described in section 2. The different models investigated are detailed in section 3. The LES results are then compared to the DNS results in section 4. Comparisons are made with the profiles of mean velocity, rms velocities and reduced (deviatoric) turbulence intensities. The main conclusions are summarized in section 5.

2. Projection test operator

The operator $\tilde{}$ is the projection from DNS to the LES grid of cell size h. For the dynamic procedure, we further consider the test operator $\hat{}$: a projection from the LES grid of size h to a LES grid of size $2\,h$. The channel flow code being pseudo-spectral in x and z, and finite differences in y, we use, as projection, the sharp Fourier cutoff in x and z. In y, we can either do nothing (not fully consistent with the dynamic procedure) or apply a test projection using sampling. The sampling is done by retaining one value every two: from a sequence of field values $[f_1, f_2, f_3, \ldots]$ on the LES grid, we retain the sequence $[f_1, f_3, \ldots]$ on the twice coarser grid. Clearly, this corresponds to a projection: a loss of information. Then, in order to obtain projected values everywhere on the LES grid (we need them for the dynamic procedure, at least in its usual version), we use

interpolation. Using here linear interpolation, the projected field evaluated on the LES grid is $[f_1, (f_1+f_3)/2, f_3, \ldots]$.

Thus, the combined operator, $\tilde{}$ followed by $\hat{}$, is also a projection: from DNS to a LES grid of size $2h$. Therefore this has nothing to do with regular explicit filtering: in that case, information is not lost and one can always recover the original field from the filtered field using a "deconvolution" method (such as the van Cittert iterative method). This point is most important: here we perform LES with projection only, and thus without regular explicit filtering and with no need for reconstruction of the effective SFS stress.

The equations for the DNS (with $\partial_i u_i = 0$) are

$$\partial_t u_i + \partial_j \left(u_i u_j\right) + \partial_i P = \nu\, \partial_j \partial_j u_i \ . \tag{2.1}$$

Those for the LES (with $\partial_i \widetilde{u}_i = 0$) are

$$\partial_t \widetilde{u}_i + \partial_j \left(\widetilde{\widetilde{u}_i \widetilde{u}_j}\right) + \partial_j \widetilde{a}_{ij} + \partial_i \widetilde{P} = \nu\, \partial_j \partial_j \widetilde{u}_i \tag{2.2}$$

with $\widetilde{a}_{ij} = \widetilde{u_i u_j} - \widetilde{\widetilde{u}_i \widetilde{u}_j}$ the SGS stress to be modelled. Thus $\widetilde{a}_{ij}$ is the projection of $u_i u_j - \widetilde{u}_i \widetilde{u}_j$, the LES resolved part of "product of complete (DNS) fields minus product of incomplete (LES) fields".

Those for the LES at the coarser level (with $\partial_i \widehat{\widetilde{u}}_i = 0$) are

$$\partial_t \widehat{\widetilde{u}}_i + \partial_j \left(\widehat{\widetilde{\widetilde{u}}_i \widetilde{u}_j}\right) + \partial_j \widehat{\widetilde{A}}_{ij} + \partial_i \widehat{\widetilde{P}} = \nu\, \partial_j \partial_j \widehat{\widetilde{u}}_i \tag{2.3}$$

with $\widehat{\widetilde{A}}_{ij} = \widehat{\widetilde{u_i u_j}} - \widehat{\widetilde{\widetilde{u}}_i \widetilde{u}_j}$ the SGS stress at the test level.

Projection, using $\hat{}$, of the equations for $\widetilde{u}_i$ leads to equations that must be consistent with those for $\widehat{\widetilde{u}}_i$. This provides the Germano's identity:

$$\widehat{\widetilde{A}}_{ij} - \widehat{\widetilde{a}}_{ij} = \widehat{\widetilde{\widetilde{u}_i \widetilde{u}_j}} - \widehat{\widetilde{\widetilde{\widetilde{u}}_i \widetilde{u}_j}} = \widehat{\widetilde{L}}_{ij} \ . \tag{2.4}$$

3. Investigated models

3.1. *Dynamic Smagorinsky model*

We first consider the dynamic Smagorinsky model. The model for the SGS stress is taken as

$$\widetilde{a}_{ij}^{M} = -2\, C \Delta^2 \left|\widetilde{S}\right| \widetilde{S}_{ij} \tag{3.1}$$

with $\widetilde{S}_{ij} = \left(\partial_j \widetilde{u}_i + \partial_i \widetilde{u}_j\right)/2$ the rate of strain tensor and $\left|\widetilde{S}\right| = \left(2 \widetilde{S}_{kl} \widetilde{S}_{kl}\right)^{1/2}$. For consistency, the model for the SGS stress at the coarser level is taken as

$$\widehat{\widetilde{A}}_{ij}^{M} = -2\, C (2\Delta)^2 \left|\widehat{\widetilde{\widetilde{u}}}\right| \widehat{\widetilde{S}}_{ij} \ . \tag{3.2}$$

The dynamic procedure consists in minimizing the error in Germano's identity,

$$\widehat{\widetilde{E}}_{ij} = \widehat{\widetilde{L}}_{ij} - \left(\widehat{\widetilde{A}}_{ij}^{M} - \widehat{\widetilde{a}}_{ij}^{M}\right) = \widehat{\widetilde{L}}_{ij} - C\Delta^2 \left(2 \left|\widehat{\widetilde{S}}\right| \widehat{\widetilde{S}}_{ij} - 8 \left|\widehat{\widetilde{\widetilde{S}}}\right| \widehat{\widetilde{\widetilde{S}}}_{ij}\right)$$

$$= \widehat{\widetilde{L}}_{ij} - C\Delta^2\, \widehat{\widetilde{Q}}_{ij} \; . \tag{3.3}$$

Minimizing $\langle \widehat{\widetilde{E}}_{ij} \widehat{\widetilde{E}}_{ij} \rangle$ in the least-square sense (where $\langle\ \rangle$ stands for averaging over the homogeneous directions: x and z for the channel flow) leads to

$$(C\Delta^2)(y) = \frac{\langle \widehat{\widetilde{L}}_{ij} \widehat{\widetilde{Q}}_{ij} \rangle}{\langle \widehat{\widetilde{Q}}_{ij} \widehat{\widetilde{Q}}_{ij} \rangle} \; . \tag{3.4}$$

3.2. *Dynamic "Smagorinsky + hyperviscosity" model*

We consider a model which combines viscosity (Smagorinsky) and a fourth-order hyperviscosity. The model for the SGS stress is here taken as

$$\widetilde{a}_{ij}^M = -2\, C\Delta^2 \widetilde{\left|\widetilde{S}\right| \widetilde{S}}_{ij} + 2\, D\Delta^4 \widetilde{\left|\widetilde{S}\right| \nabla^2 \widetilde{S}}_{ij} \; . \tag{3.5}$$

The model for the SGS stress at the coarser level is thus

$$\widehat{\widetilde{A}}_{ij}^M = -2\, C(2\Delta)^2 \widehat{\widetilde{\left|\widetilde{S}\right| \widetilde{S}}}_{ij} + 2\, D(2\Delta)^4 \widehat{\widetilde{\left|\widetilde{S}\right| \nabla^2 \widetilde{S}}}_{ij} \; , \tag{3.6}$$

and the error is

$$\begin{aligned} \widehat{\widetilde{E}}_{ij} &= \widehat{\widetilde{L}}_{ij} - C\Delta^2 \left(2 \widehat{\widetilde{\left|\widetilde{S}\right| \widetilde{S}}}_{ij} - 8 \widehat{\widetilde{\left|\widetilde{S}\right| \widetilde{S}}}_{ij} \right) + D\Delta^4 \left(2 \widehat{\widetilde{\left|\widetilde{S}\right| \nabla^2 \widetilde{S}}}_{ij} - 32 \widehat{\widetilde{\left|\widetilde{S}\right| \nabla^2 \widetilde{S}}}_{ij} \right) \\ &= \widehat{\widetilde{L}}_{ij} - C\Delta^2\, \widehat{\widetilde{Q}}_{ij} + D\Delta^4\, \widehat{\widetilde{W}}_{ij} \; . \end{aligned} \tag{3.7}$$

Minimizing the error leads to the following system for determining $C\Delta^2$ and $D\Delta^4$ as function of y:

$$\begin{aligned} \langle \widehat{\widetilde{Q}}_{ij} \widehat{\widetilde{Q}}_{ij} \rangle\, (C\Delta^2) - \langle \widehat{\widetilde{Q}}_{ij} \widehat{\widetilde{W}}_{ij} \rangle\, (D\Delta^4) &= \langle \widehat{\widetilde{L}}_{ij} \widehat{\widetilde{Q}}_{ij} \rangle \\ -\langle \widehat{\widetilde{Q}}_{ij} \widehat{\widetilde{W}}_{ij} \rangle\, (C\Delta^2) + \langle \widehat{\widetilde{W}}_{ij} \widehat{\widetilde{W}}_{ij} \rangle\, (D\Delta^4) &= -\langle \widehat{\widetilde{L}}_{ij} \widehat{\widetilde{W}}_{ij} \rangle \; . \end{aligned} \tag{3.8}$$

3.3. *Dynamic Smagorinsky model using a "small field": a regularized multiscale model*

The model by Hiughes *et al.* (2001a) corresponds to limiting the Smagorinsky model to the small scales. The model has zero effect at large scales, and is an effective viscosity at small scales. In our regularized version of the model (Winckelmans *et al.* (2001a)), we achieve this by applying the dynamic Smagorinsky model to a regularized "small-scales field" obtained as

$$\widetilde{u}_i^s = \widetilde{u}_i - \overline{\widetilde{u}}_i \tag{3.9}$$

with $\overline{\widetilde{u}}_i = \overline{G} * \widetilde{u}$ where $\overline{G}$ is a regular smoothing filter with a Fourier transform that goes to zero at the LES cutoff wavenumber. A convenient second-order filter is the compact discrete filter (thus easily applied in physical space). In one-dimension (1-D) it reads

$$\overline{f}(x) = f(x) + \left(f(x+h) - 2f(x) + f(x-h)\right)/4 = \left(I + \delta^2/4\right) f(x) \; . \tag{3.10}$$

In Fourier space, this gives

$$\overline{\mathcal{G}}(k) = 1 - \frac{1}{2}\left(1 - \cos(kh)\right) = 1 - \sin^2(kh/2) \; . \tag{3.11}$$

In 3-D, it is applied one direction at a time,

$$\overline{\widetilde{u}}_i = \left(I + \delta_x^2/4\right)\left(I + \delta_y^2/4\right)\left(I + \delta_z^2/4\right)\widetilde{u}_i \;, \tag{3.12}$$

so that

$$\widetilde{u}_i^s = \widetilde{u}_i - \left(I + \delta_x^2/4\right)\left(I + \delta_y^2/4\right)\left(I + \delta_z^2/4\right)\widetilde{u}_i \;. \tag{3.13}$$

The model for the SGS stress is thus taken as

$$\widetilde{a}_{ij}^M = -2\,C\Delta^2\,\widetilde{\left|\widetilde{S}\right|\widetilde{S}_{ij}^s} \tag{3.14}$$

where $\widetilde{S}_{ij}^s = \left(\partial_j\widetilde{u}_i^s + \partial_i\widetilde{u}_j^s\right)/2$.

Notice that higher-order filters can easily be constructed by iterating the second-order filter, thus still only requiring a stencil-3 wide discrete operation in each direction; see Winckelmans *et al.* (2001a). For instance, the fourth order filter used in Stolz *et al.* (2001),

$$\overline{f}(x) = f(x) + \left(-f(x+2h) + 4f(x+h) - 6f(x) + 4f(x-h) - f(x-2h)\right)/16 \tag{3.15}$$

and

$$\overline{\mathcal{G}}(k) = 1 - \left(3 - 4\cos(kh) + \cos(2kh)\right)/8 = 1 - \left(\sin^2(kh/2)\right)^2 \tag{3.16}$$

is also obtainable from

$$\overline{f}(x) = \left(I - \left(-\delta^2/4\right)^2\right) f(x) \;. \tag{3.17}$$

Equivalently, a filter of order $2n$ is obtained from:

$$\overline{f}(x) = \left(I - \left(-\delta^2/4\right)^n\right) f(x) \;, \tag{3.18}$$

leading to

$$\overline{\mathcal{G}}(k) = 1 - \left(\sin^2(kh/2)\right)^n \;. \tag{3.19}$$

3.4. *Dynamic Smagorinsky model using an "enhanced field"*

Another view is to consider a model that is viscosity-like at large scales and more effective at small scales. This is easily done by using the dynamic Smagorinsky model applied to an artificial "enhanced field", see Winckelmans *et al.* (2001a). In the present implementation, $\widetilde{u}_i$ is replaced by

$$\widetilde{u}_i^e = \left[I + (I - \overline{G})\right] * \widetilde{u}_i = 2\widetilde{u}_i - \overline{\widetilde{u}}_i \;. \tag{3.20}$$

The model for the SGS stress is thus

$$\widetilde{a}_{ij}^M = -2\,C\Delta^2\,\widetilde{\left|\widetilde{S}\right|\widetilde{S}_{ij}^e} \tag{3.21}$$

where $\widetilde{S}_{ij}^e = \left(\partial_j\widetilde{u}_i^e + \partial_i\widetilde{u}_j^e\right)/2$. Again, we here use the discrete filter, leading to

$$\widetilde{u}_i^e = 2\widetilde{u}_i - \left(I + \delta_x^2/4\right)\left(I + \delta_y^2/4\right)\left(I + \delta_z^2/4\right)\widetilde{u}_i \;. \tag{3.22}$$

Clearly, the model essentially behaves as a a fourth-order hyperviscosity at the small scales.

4. Results

The turbulent channel flow at $\mathrm{Re}_\tau = 395$ was investigated, with the different SGS models but using the same LES code (thus allowing for self-consistent comparisons between the models). The reference DNS is that of Moser *et al.* (1999). The code is based

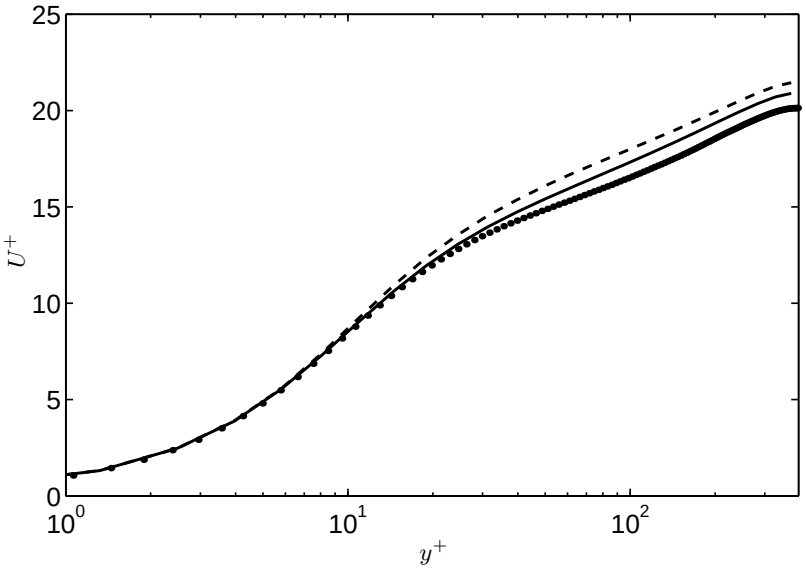

FIGURE 1. Mean velocity: dynamic Smagorinsky model without (solid) and with sampling + interpolation in y (dash); DNS data (solid circles).

on a pseudo-spectral method in the streamwise, x, and spanwise, z, directions, and on fourth-order spectral-like compact finite differences in the wall-normal direction, y. The flow is driven by a constant mean pressure gradient. A semi-implicit second order time integration scheme is used. The grid is stretched in y using a hyperbolic tangent function with a stretching factor of 2.75. The grid resolution is set to (64x49x48) giving, after de-aliasing, a resolved grid of (42x49x32). Preliminary runs were carried out with a grid of (72x37x54) points, but the resolution in the wall-normal direction proved to be too small to correctly capture the mean-velocity profile in the transition region. The x and z resolutions were here also adapted to join in an effort of comparisons between different codes on this particular flow, in collaboration with J. Gullbrand and F. K. Chow (whose work is reported elsewhere in this volume).

4.1. *Projection test operator in y*

The dynamic procedure with a sampling procedure in y at the test level is more consistent with the similarity hypothesis between the models at the LES grid and test levels. Better results were thus expected. However, the results were worse for all models when the sampling procedure in y was applied.

The results for the case of the dynamic Smagorinsky model are shown in figures 1 and 2. Both the mean velocity profile and the rms velocities are closer to the DNS data when no "sampling + interpolation" is applied in y as part of the test projection operation. This conclusion is also valid for the results obtained with the other models (not shown here).

Those results have two consequences. The first one is the ineffectiveness of the sampling + interpolation procedure as a substitute to a true coarser discretization at the test level. The interpolation applied to maintain the information datn all LES grid points creates spurious information at high wavenumbers instead of preserving the cutoff effect of the sampling procedure. This has a negative impact on the dynamic determination

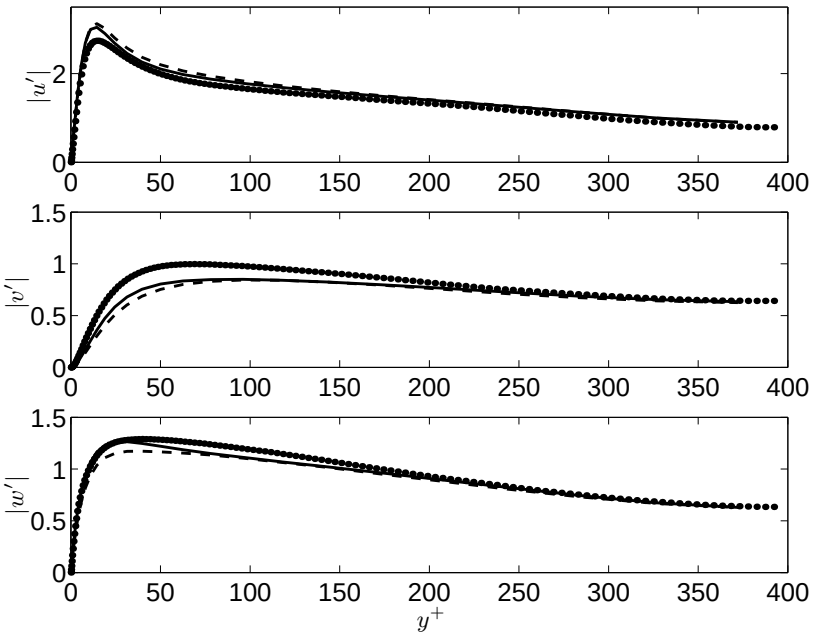

FIGURE 2. rms velocities: dynamic Smagorinsky model without (solid) and with sampling + interpolation in y (dash); DNS data (solid circles).

of the model coefficient(s), and hence on the results obtained. One way to avoid this interpolation issue would be to use sampling only, and thus to evaluate the dynamic coefficient on the test-filtered (twice coarser) grid only. One would then interpolate the dynamic coefficient back to the LES grid. This requires the definition of all the operators (derivatives, products, etc.) at both the LES and test grid levels, and was not considered in the present work (due to lack of time). The second consequence is the relatively small impact of the two dynamic implementations on the mean results. The impact on the value of the dynamic coefficient is however higher, with a maximal difference of roughly 60% in the center of the channel.

The following results all correspond to a dynamic procedure without sampling + interpolation in the wall-normal direction.

4.2. *Comparison of the models*

The mean velocity profiles obtained with the different models are presented in figures 3 and 4. The regularized version of the Hughes *et al.* model performs best. See also the good results reported in Hughes *et al.* (2001b) for decaying isotropic turbulence, and in Hiughes *et al.* (2001a) for channel flow. This conclusion is however slightly contradictory to the results obtained for more challenging (coarser grid) runs for decaying isotropic turbulence in Winckelmans *et al.* (2001a). In that case, the lack of model dissipation at the large scales was more crucial.

The results obtained with the dynamic model Smagorinsky + hyperviscosity are encouraging: the dynamic procedure was indeed successful in determining the two dynamic coefficients. They are however also disappointing: the results are no better than those obtained using the dynamic Smagorinsky model alone. This is explained by the close correspondence between the dynamic coefficients obtained for the Smagorinsky term. The

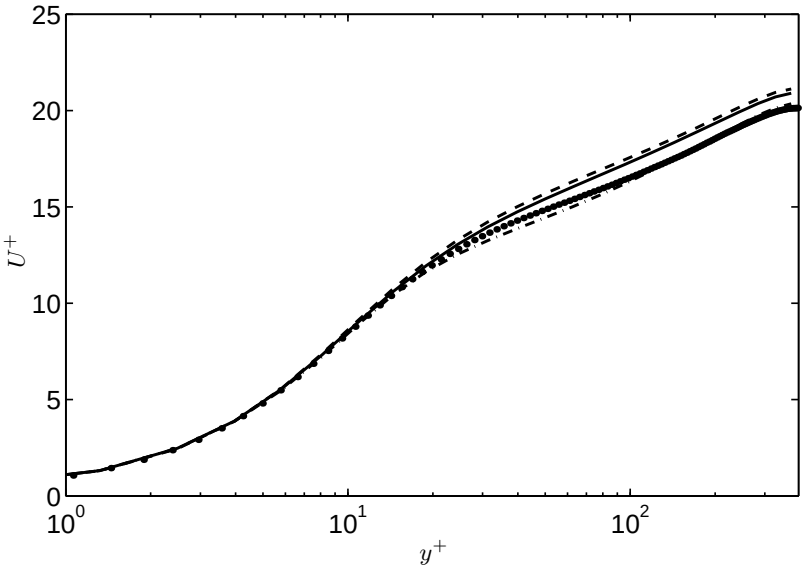

FIGURE 3. Mean velocity: dynamic Smagorinsky model (solid); dynamic Smagorinsky + hyperviscosity model (dash); regularized version of Hughes model (chained dot); DNS data (solid circles).

coefficients are similar up to $y^+ \approx 100$. The coefficient $(C\Delta^2)$ for the Smagorinky model alone goes up to 1.0×10^{-4} in the center region, while it goes to 0.6×10^{-4} with the added hyperviscosity term. This lower value is compensated by the dissipation of the hyperviscosity term, leading to nearly identical results for the mean velocity profiles.

Better results are obtained when using the Smagorinsky model applied to the artificially enhanced velocity field, see figure 4.

The conclusions drawn from the mean-velocity profiles are also valid for the rms velocities, see figures 5 and 6. The regularized Hughes model performs best. It correctly reproduces the streamwise and normal rms velocities, yet it produces an overshoot of the maximum near-wall value for the spanwise component. Similar behavior is reported by Hughes *et al.* (2001b). The results for the Smagorinsky model and the Smagorinsky + hyperviscosity model are essentially the same. Finally, the results for the Smagorinsky model applied to an enhanced field are also quite good: this new model is promising.

However, the comparison of the rms velocities from the DNS with those calculated from the LES (including the LES model contribution) is not entirely valid. Indeed, since the SGS models, $\widetilde{a}_{ij}^M$, used here have a zero trace, one can only reconstruct, and thus fairly compare with DNS, the deviatoric part of the Reynolds stress tensor, see Winckelmans *et al.* (2002). Recall also that the trace of the Reynolds stress tensor is the DNS turbulent kinetic energy, which is different from the resolved LES turbulent kinetic energy. The fair comparison, on the deviatoric components, consists in comparing $R_{ij}^{DNS^*}$ (where * means the reduced (traceless) part of the tensor) to $R_{ij}^{LES^*} - \langle \widetilde{a}_{ij}^M \rangle$. The comparison on the diagonal components (the "reduced turbulence intensities"), is presented in figure 7. The previously drawn conclusions remain unchanged. This is so because, in the present case, the resolved LES turbulent kinetic energy is still close to the DNS turbulent kinetic energy.

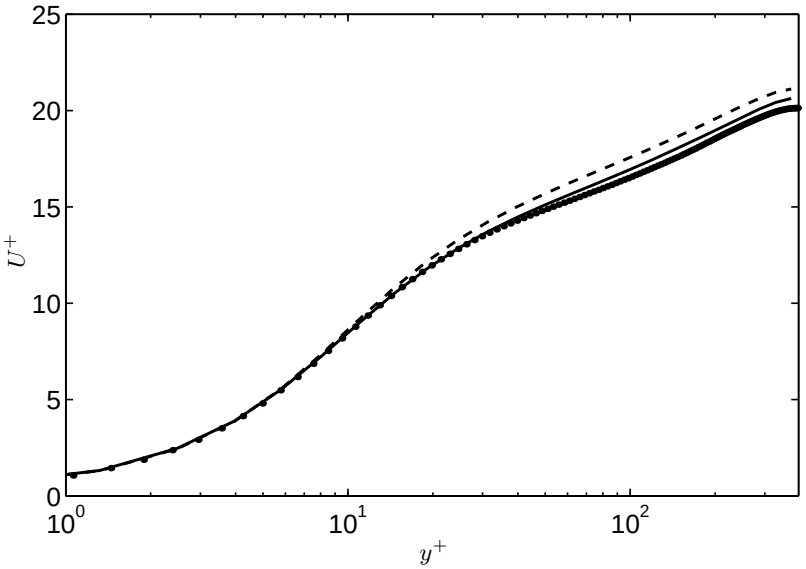

FIGURE 4. Mean velocity: dynamic Smagorisnky model applied to enhanced velocity field (solid); dynamic Smagorinsky + hyperviscosity model (dash); DNS data (solid circles).

5. Conclusions

The assessment of some recent LES models carried out for decaying isotropic turbulence was here extended to channel flow at $\mathrm{Re}_\tau = 395$.

Three models were investigated in addition to the Smagorinsky model: a regularized version of the model by Hughes *et al.*, a Smagorinsky + hyperviscosity model, and a Smagorinsky model acting on an artificially enhanced velocity field. A dynamic version of each model was developed and implemented.

A particular implementation of the dynamic procedure was also considered, where "sampling followed by interpolation" is applied as a test projection in the wall-normal direction (in addition to the usual test projection in the homogeneous directions using the sharp cutoff in spectral space). No improvement in the results was obtained. It was argued that the interpolation creates spurious information at high wavenumbers on top of the cutoff effect achieved by the sampling. Another method that avoids the interpolation part was proposed (not tested yet).

Significant improvements in the profiles of mean velocity, rms velocities, and reduced turbulence intensities, as compared to the Smagorinsky model, are obtained when using the model of Hughes et al., and when using the Smagorinsky model acting on an artificially enhanced velocity field. The results obtained using the Smagorinsky + hyperviscosity model are somewhat disappointing as no clear benefit is seen on the mean profiles. The benefit of this model could possibly lie in better agreement with DNS data on other quantities (such as two-point correlations and spectra). This deserves further investigation.

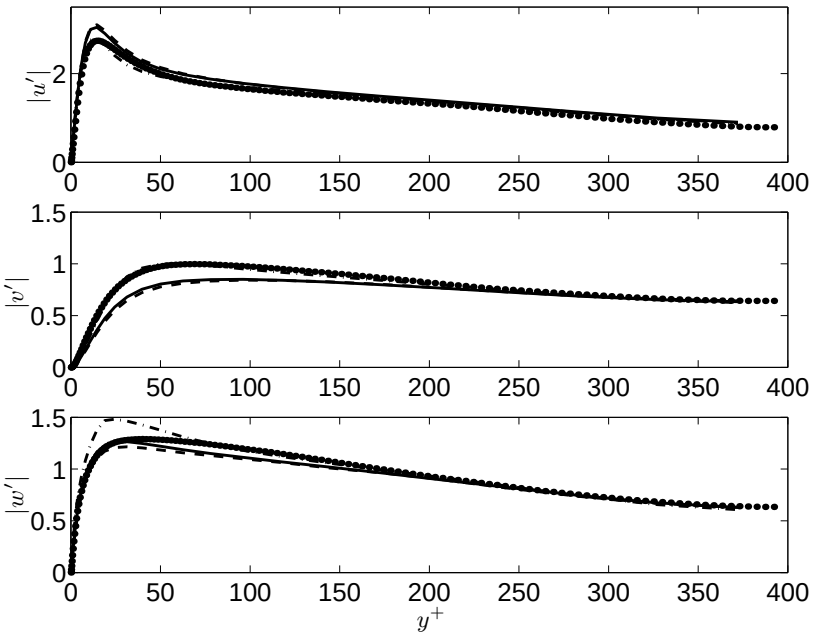

FIGURE 5. rms velocities: dynamic Smagorinsky model (solid); dynamic Smagorinsky + hyperviscosity model (dash); regularized version of Hughes model (chained dot); DNS data (solid circles).

Acknowledgments

Thanks are extended to Dr. J. Gullbrand and F. K. Chow who contributed to this work through many useful discussions (see also their paper elsewhere in this volume). Thanks are also due to Prof. J. Ferziger for his input and encouragement concerning the dynamic model "Smagorinsky + hyperviscosity", and to Prof. R. Street for useful discussions about explicit filtering in LES.

REFERENCES

CARATI, D., WINCKELMANS, G. S. & JEANMART, H. 2001 On the modelling of the subgrid-scale and filtered-scale stress tensors in large-eddy simulation. *J. Fluid Mech.* **441**, 119–138.

GERMANO, M., PIOMELLI, U., MOIN, P. & CABOT, W. 1991 A dynamic subgrid-scale eddy-viscosity model. *Phys. Fluids A* **3**, 1760–1765.

GHOSAL, S., LUND, T. S. & MOIN, P. 1992 A local dynamic model for large-eddy simulation. *Annual Research Briefs*, Center for Turbulence Research, NASA Ames/Stanford Univ., 3–25.

GHOSAL, S., LUND, T. S., MOIN, P. & AKSELVOLL, K. 1995 A dynamic localization model for large-eddy simulation of turbulent flows. *J. Fluid Mech.* **286**, 229–255.

HUGHES, T. J. R., MAZZEI, L., OBERAI, A. A. & WRAY, A. A. 2001a The multiscale formulation of large eddy simulation: Decay of homogeneous isotropic turbulence. *Phys. Fluids* **13**, 505–512.

HUGHES, T. J. R., OBERAI, A. A. & MAZZEI, L. 2001b Large eddy simulation of

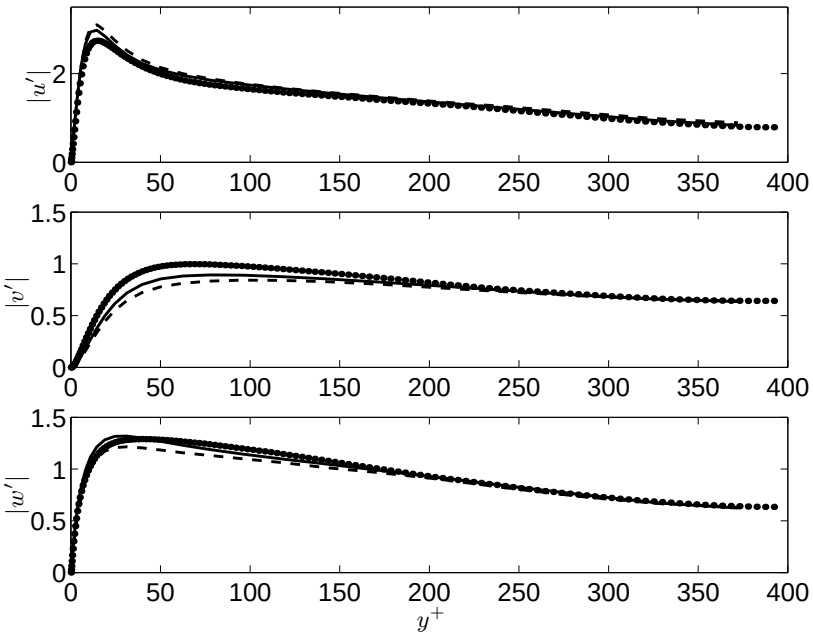

FIGURE 6. rms velocities: dynamic Smagorinsky model applied to an enhanced velocity field (solid); dynamic Smagorinsky + hyperviscosity model (dash); DNS data (solid circles).

turbulent channel flow by the variational multiscale method. *Phys. Fluids* **13**, 1784–1799.

MÉTAIS, O. & LESIEUR, M. 1992 Spectral large-eddy simulation of isotropic and stably stratified turbulence. *J. Fluid Mech.* **239**, 157–194.

MOSER, R. D., KIM, J. & MANSOUR, N. N. 1999 Direct numerical simulation of turbulent channel flow up to $\mathrm{Re}_\tau = 590$. *Phys. Fluids* **11**, 943–945.

SMAGORINSKY, J. 1963 General circulation experiments with the primitive equations. *Mon. Weather Rev.* **91**, 99–164.

STOLZ, S. & ADAMS, N. A. 1999 An approximate deconvolution procedure for large-eddy simulation. *Phys. Fluids* **11**, 1699–1701.

STOLZ, S., ADAMS, N. A. & KLEISER, L. 2001 An approximate deconvolution model for large-eddy simulation with application to incompressible wall-bounded flows. *Phys. Fluids* **13**, 997–1015.

WINCKELMANS, G. S., WRAY, A. A., VASILYEV, O. V. & JEANMART, H. 2001 Explicit-filtering large-eddy simulation using the tensor-diffusivity model supplemented by a dynamic Smagorinsky term. *Phys. Fluids* **13**, 1385-1403.

WINCKELMANS, G. S. & JEANMART, H. 2001 Assessment of some models for LES without and with explicit filtering. *Direct and Large-Eddy Simulation IV*(B.J. Geurts, R. Friedrich and O. Métais, eds.), ERCOFTAC Series **8**, Kluwer, pp. 55–66.

WINCKELMANS, G. S., CARATI, D, & JEANMART, H. 2002 On the comparison of turbulence intensities from large-eddy simulation with those from experiment or direct numerical simulation, Brief Comm., *Phys. Fluids* **14**, 1809-1811.

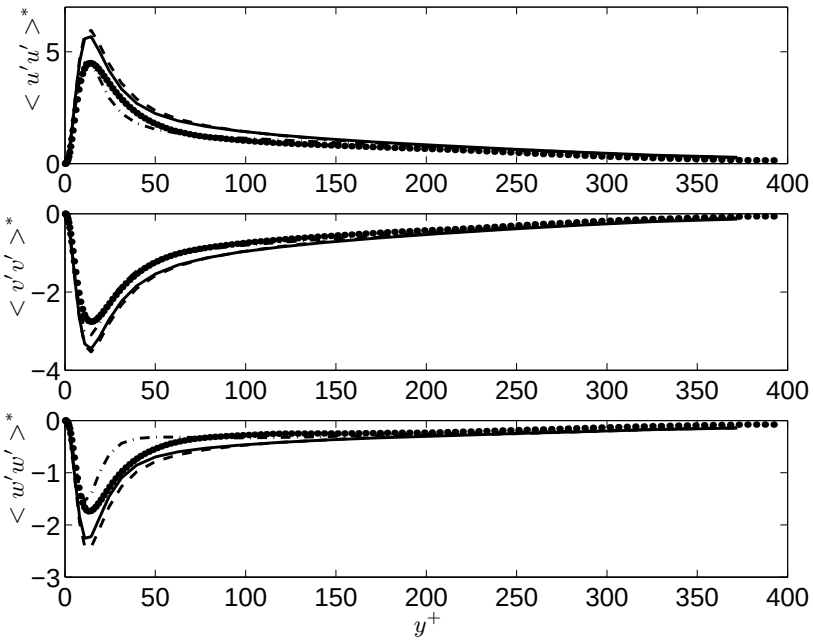

FIGURE 7. Reduced turbulence intensities: dynamic Smagorinsky model (solid); dynamic Smagorinsky + hyperviscosity model (dash); regularized version of Hughes model (chained dot); DNS data (solid circles).